response to a 90° grating from that to a 0° grating. For stimuli undergoing non-orthogonal motion, both the orientation and the axis of motion were different by 90° between the subtracted stimuli. For example, the response to a texture with 45° oriented bars moving horizontally was subtracted from the response to a texture with 135° oriented bars moving vertically. Results obtained with difference imaging were verified with single-condition imaging by subtracting the response to a blank screen from the stimulus-driven response (see Supplementary Fig. 6).

Optical map analysis

To interpret the patterns of activity evoked by various stimulus configurations, we developed a population response profile that captured the relative activation of each pixel in the region of interest and expressed these values in terms of the pixel's preferred orientation assessed with gratings. Grating images obtained for four to eight orientations were low-pass and high-pass filtered and vector-summed to produce referent grating-angle maps[9]. To compute a population response profile for a given stimulus, the difference image for that stimulus was assigned a threshold at the mean grey value and each pixel above the threshold was weighted (greyscale value minus threshold). On the basis of each pixel's preferred grating orientation, the weighted pixel values were summed into nine 20° angle bins (from 0° to 180°) and normalized to the highest count across conditions (for example, across length or speed). The resulting histograms were fitted with gaussian functions and the peak and width of the response were determined along with the R^2 value of the best-fit gaussian function. For direct comparison between any two images, the two-dimensional correlation coefficient (R) between the two (high-pass and low-pass filtered) images was determined with the Matlab Image Processing Toolbox (Mathworks, Natick, Massachusetts). This value was then squared and reported as the more intuitive coefficient of determination (R^2).

Difference images shown in figures were high-pass filtered and a region of interest was selected for demonstration purposes. The region of interest was selected as the region of the image that showed both a strong response and a representative shift with change in stimulus conditions. Contour overlays were prepared by superimposing iso-orientation contours from a referent grating-angle map over a filtered and re-clipped (to ± 2 s.d.) texture, dot or grating difference image.

Electrophysiology

Single and multiple units were recorded extracellularly from V1 with a tungsten microelectrode (impedance 8–14 MΩ). Action potentials were recorded from the superficial layers (<400 μm) and discriminated by using Spike2 software (Cambridge Electronic Design, Cambridge, UK). Orientation and direction tuning functions were obtained for each site by panning a bar (40° × 0.4°) across the receptive field. Tuning curves for textures or dots were obtained by panning full-field textures (at eight orientations) or a field of dots in 16 directions (at 22.5° intervals). For non-orthogonal motion, the offset between bar orientation and direction of motion was 45°. For the single-bar experiments, the centre and size of the minimal discharge field were determined by using a small orthogonally drifting bar. A square-wave bar of varying length was then moved non-orthogonally such that it always passed through the centre of the receptive field. In some cases, 3–10 speeds were randomized within the direction tuning experiment. Action potentials were counted for the entire stimulus duration (1–2 s). Offline spike sorting and tuning analysis was performed with custom-written Spike2 software.

Received 13 January; accepted 23 April 2003; doi:10.1038/nature01721.

1. Hubel, D. H. & Wiesel, T. N. Ferrier Lecture: Functional architecture of macaque monkey visual cortex. *Proc. R. Soc. Lond. B* **198,** 1–59 (1977).
2. Hubener, M., Shoham, D., Grinvald, A. & Bonhoeffer, T. Spatial relationships among three columnar systems in cat area 17. *J. Neurosci.* **17,** 9270–9284 (1997).
3. Swindale, N. V. How many maps are there in visual cortex? *Cereb. Cortex* **10,** 633–643 (2000).
4. Swindale, N. V., Shoham, D., Grinvald, A., Bonhoeffer, T. & Hubener, M. Visual cortex maps are optimized for uniform coverage. *Nature Neurosci.* **3,** 822–826 (2000).
5. Issa, N. P., Trepel, C. & Stryker, M. P. Spatial frequency maps in cat visual cortex. *J. Neurosci.* **20,** 8504–8514 (2000).
6. Everson, R. M., Prashanth, A. K., Gabbay, M., Knight, B. W., Sirovich, L. & Kaplan, E. Representation of spatial frequency and orientation in the visual cortex. *Proc. Natl Acad. Sci. USA* **95,** 8334–8338 (1998).
7. Shmuel, A. & Grinvald, A. Functional organization for direction of motion and its relationship to orientation maps in cat area 18. *J. Neurosci.* **16,** 6945–6964 (1996).
8. Weliky, M., Bosking, W. H. & Fitzpatrick, D. A systematic map of direction preference in primary visual cortex. *Nature* **379,** 725–728 (1996).
9. Bonhoeffer, T. & Grinvald, A. in *Brain Mapping: The Methods* (eds Toga, A. W. & Mazziotta, J. C.) 55–97 (Academic, New York, 1996).
10. Wuerger, S., Shapley, R. & Rubin, N. 'On the visually perceived direction of motion' by Hans Wallach, 60 years later. *Perception* **25,** 1317–1367 (1996).
11. Adelson, E. H. & Movshon, J. A. Phenomenal coherence of moving visual patterns. *Nature* **300,** 523–525 (1982).
12. De Valois, R. L. & De Valois, K. K. *Spatial Vision* (Oxford Univ. Press, New York, 1988).
13. Lorenceau, J., Shiffrar, M., Wells, N. & Castet, E. Different motion sensitive units are involved in recovering the direction of moving lines. *Vision Res.* **33,** 1207–1217 (1993).
14. Pack, C. C. & Born, R. T. Temporal dynamics of a neural solution to the aperture problem in visual area MT of macaque brain. *Nature* **409,** 1040–1042 (2001).
15. Shoham, D., Hubener, M., Schulze, S., Grinvald, A. & Bonhoeffer, T. Spatio-temporal frequency domains and their relation to cytochrome oxidase staining in cat visual cortex. *Nature* **385,** 529–533 (1997).
16. Hubel, D. H. & Wiesel, T. N. Receptive fields and functional architecture in two non-striate visual areas (18 and 19) of the cat. *J. Neurophysiol.* **28,** 229–289 (1965).
17. Gilbert, C. D. Laminar differences in receptive field properties of cells in cat primary visual cortex. *J. Physiol. (Lond.)* **268,** 391–421 (1977).
18. Skottun, B. C., Zhang, J. & Grosof, D. H. On the direction selectivity of cells in the visual cortex to drifting dot patterns. *Vis. Neurosci.* **11,** 885–897 (1994).
19. Movshon, J. A., Thompson, I. D. & Tolhurst, D. J. Spatial summation in the receptive fields of simple cells in the cat's striate cortex. *J. Physiol. (Lond)* **283,** 53–77 (1978).
20. Movshon, J. A., Thompson, I. D. & Tolhurst, D. J. Receptive field organization of complex cells in the cat's striate cortex. *J. Physiol. (Lond.)* **283,** 79–99 (1978).
21. De Valois, K. K., De Valois, R. L. & Yund, E. W. Responses of striate cortex cells to grating and checkerboard patterns. *J. Physiol. (Lond.)* **291,** 483–505 (1979).
22. Gizzi, M. S., Katz, E., Schumer, R. A. & Movshon, J. A. Selectivity for orientation and direction of motion of single neurons in cat striate and extrastriate visual cortex. *J. Neurophysiol.* **63,** 1529–1543 (1990).
23. Hammond, P. & Smith, A. T. Directional tuning interactions between moving oriented and textured stimuli in complex cells of feline striate cortex. *J. Physiol. (Lond.)* **342,** 35–49 (1983).
24. Skottun, B. C., Grosof, G. H. & De Valois, R. L. Responses of simple and complex cells to random dot patterns: a quantitative comparison. *J. Neurophysiol.* **59,** 1719–1735 (1988).
25. Geisler, W. S., Albrecht, D. G., Crane, A. M. & Stern, L. Motion direction signals in the primary visual cortex of cat and monkey. *Vis. Neurosci.* **18,** 501–516 (2001).
26. Galuske, R. A. W., Schmidt, K. E., Kluge, T. & Singer, W. Motion and velocity representation in cat primary visual cortex. *Soc. Neurosci. Abstr.* vol. 27. Program No. 164.2 (2001).
27. Carandini, M., Heeger, D. J. & Movshon, J. A. in *Cerebral Cortex* (ed. Ulinski, P. S.) vol. 13, 401–443 (Kluwer Academic/Plenum, New York, 1999).
28. Adelson, E. H. & Bergen, J. R. Spatiotemporal energy models for the perception of motion. *J. Opt. Soc. Am. A* **2,** 284–299 (1985).
29. White, L. E., Bosking, W. H., Williams, S. M. & Fitzpatrick, D. Maps of central visual space in ferret V1 and V2 lack matching inputs from the two eyes. *J. Neurosci.* **19,** 7089–7099 (1999).

Supplementary Information accompanies the paper on **www.nature.com/nature**.

Acknowledgements We thank D. Purves, J. A. Movshon, S. Nundy, J. C. Crowley and members of the Fitzpatrick laboratory for helpful discussions. This work was supported by a grant from the National Institutes of Health to D.F.

Competing interests statement The authors declare that they have no competing financial interests.

Correspondence and requests for materials should be addressed to D.F. (fitzpat@neuro.duke.edu).

Cyclic AMP/GMP-dependent modulation of Ca^{2+} channels sets the polarity of nerve growth-cone turning

Makoto Nishiyama*, Akemi Hoshino*, Lily Tsai*, John R. Henley†, Yoshio Goshima‡, Marc Tessier-Lavigne§, Mu-ming Poo† & Kyonsoo Hong*

** Department of Biochemistry, New York University School of Medicine, New York, New York 10016-6402, USA*
† Division of Neurobiology, Department of Molecular and Cell Biology, University of California at Berkeley, Berkeley, California 94720-3200, USA
‡ Department of Molecular Pharmacology and Neurobiology, Yokohama City University School of Medicine, Yokohama 236-0004, Japan
§ Howard Hughes Medical Institute, Department of Biological Sciences, Stanford University, Stanford, California 94305-5020, USA

Signalling by intracellular second messengers such as cyclic nucleotides and Ca^{2+} is known to regulate attractive and repulsive guidance of axons by extracellular factors[1,2]. However, the mechanism of interaction among these second messengers in determining the polarity of the guidance response is largely unknown. Here, we report that the ratio of cyclic AMP to cyclic GMP activities sets the polarity of netrin-1-induced axon guidance: high ratios favour attraction, whereas low ratios favour repulsion. Whole-cell recordings of Ca^{2+} currents at *Xenopus* spinal neuron growth cones indicate that cyclic nucleotide signalling directly modulates the activity of L-type Ca^{2+} channels

© 2003 Nature Publishing Group

(LCCs) in axonal growth cones. Furthermore, cGMP signalling activated by an arachidonate 12-lipoxygenase metabolite[3] suppresses LCC activity triggered by netrin-1, and is required for growth-cone repulsion mediated by the DCC–UNC5 receptor complex[4]. By linking cAMP and cGMP signalling and modulation of Ca^{2+} channel activity in growth cones, these findings delineate an early membrane-associated event responsible for signal transduction during bi-directional axon guidance.

A gradient of netrin-1 induces chemoattraction of *Xenopus* spinal neuron growth cones by means of the netrin-1 receptor deleted in colorectal cancer (DCC)[5], whereas overexpression of another netrin-1 receptor (UNC5) in these neurons causes netrin-1 to induce chemorepulsion through the DCC–UNC5 receptor complex[4]. In neurons not overexpressing UNC5, the DCC-mediated attraction is converted to repulsion when cAMP signalling is blocked by the membrane-permeable cAMP antagonist Rp-cAMPS or the protein kinase A (PKA) inhibitor KT5720 (ref. 6). The association between cyclic nucleotide signalling and DCC–UNC5-mediated repulsion is not known.

We therefore examined the relationship between cAMP and cGMP signalling on DCC-mediated attraction in control neurons, and on DCC–UNC5-mediated repulsion in UNC5H2-overexpressing neurons. In control neurons, bath application of KT5720 (200 nM) converted DCC-mediated attraction to repulsion (Fig. 1a, c)[6], and this repulsion was abolished by the membrane-permeable cGMP analogue 8-bromo-cGMP (8-Br-cGMP, 20 μM) (Fig. 1a, c). Bath-application of 8-Br-cGMP or *S*-nitroso-*N*-acetyl-penicillamine (SNAP, 300 μM), a nitric oxide donor known to elevate the cytosolic cGMP level[7], completely converted DCC-mediated attraction to repulsion (Fig. 1a, right panel, c). However, at a higher concentration of 8-Br-cGMP (100 μM), we found that the attractive response was not affected, consistent with an earlier report[8] (Supplementary Information). Thus, the modulatory effects of 8-Br-cGMP seem to be dose dependent, and netrin-1-induced turning responses might be regulated by both cAMP and cGMP. For DCC–UNC5-mediated repulsion, bath application of KT5720 abolished the repulsion induced by a netrin-1 gradient (Fig. 1b, c), although it had no significant effect on semaphorin 3A (Sema3A)-induced repulsion[8] (Fig. 1c). Furthermore, application of the protein kinase G (PKG) inhibitor KT5823 (750 nM) converted DCC–UNC5-mediated repulsion to attraction (Fig. 1b, c), whereas DCC-mediated attraction in control neurons was not significantly affected (Fig. 1c). Taken together, these results indicate that cGMP signalling has a major regulatory role in netrin-1-induced repulsion, whereas cAMP signalling modulates both DCC- and DCC–UNC5-mediated attraction and repulsion, respectively. Because cAMP signalling did not affect neuropilin-1 (NP-1)-mediated repulsion induced by Sema3A (Fig. 1c and ref. 9), the dependence on cyclic nucleotide signalling pathways might differ among different types of repulsive signals.

To address the relative roles of cAMP- and cGMP-dependent pathways in growth-cone guidance by netrin-1, we systematically varied the ratio of the membrane-permeable cyclic nucleotide analogues Sp-8-Br-cAMPS and 8-Br-cGMP, while maintaining their total concentration at 10 μM. As shown in Fig. 1d, as the ratio of the concentration of [Sp-8-Br-cAMPS]/[8-Br-cGMP]

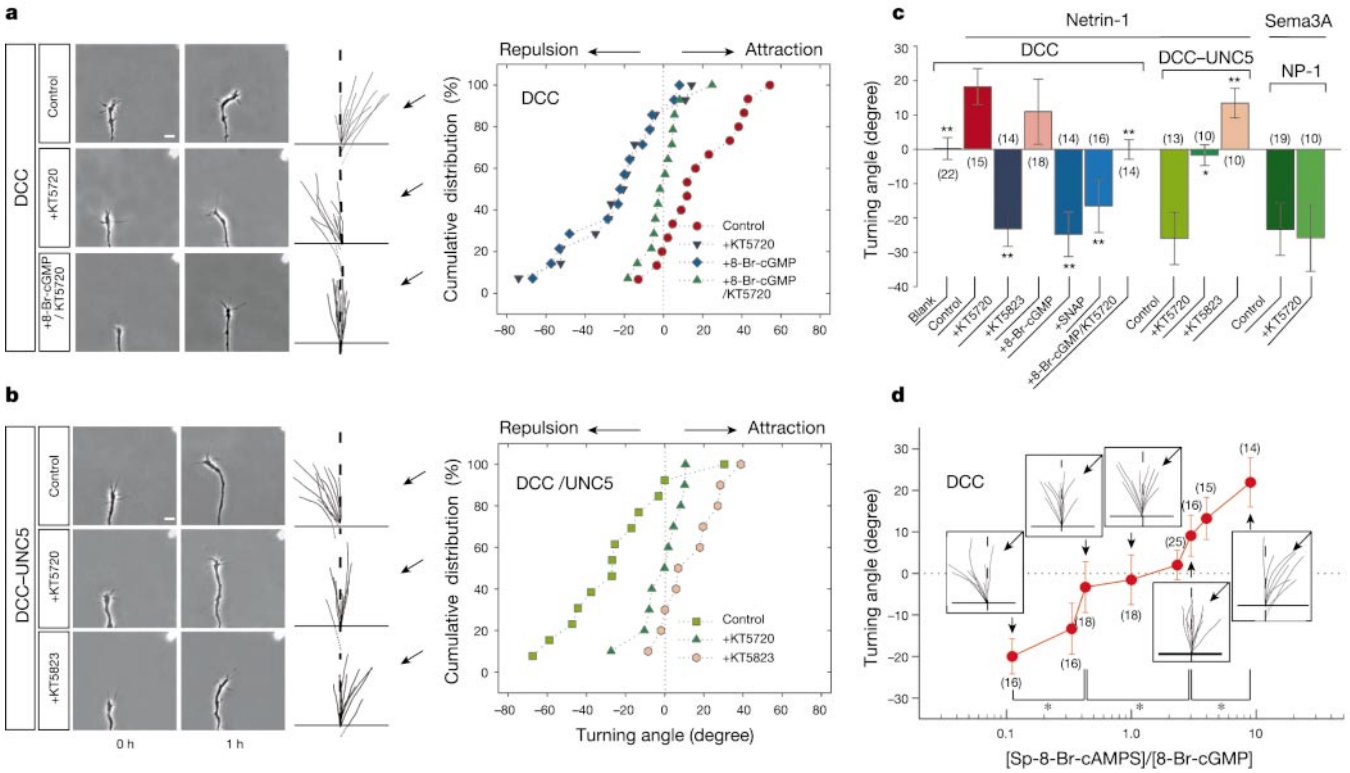

Figure 1 cAMP/cGMP signalling-dependent bi-directional growth-cone turning induced by netrin-1. **a**, **b**, Growth cones of DCC-expressing[5] (DCC) and UNC5H2-overexpressing[4] (DCC–UNC5) neurons before (0 h) and after (1 h) exposure to a netrin-1 gradient (arrows)[4] under various conditions (left panels). Traces depict the trajectories of neurite extension after each assay. The right panels show the distribution of turning angles for all neurons examined. Scale bars, 10 μm. **c**, Average turning angles for each assay. The column labelled 'blank' indicates that netrin-1 was omitted in the pipette. Significant differences from the control group are indicated (asterisk, $P < 0.05$; double asterisk, $P < 0.01$; Mann–Whitney *U*-test). **d**, Average turning angles of DCC neurons after exposure to a netrin-1 gradient at different [Sp-8-Br-cAMPS]/[8-Br-cGMP] ratios in the bath. Samples of neurite trajectories are shown (insets). Significant differences between the ratios are indicated (asterisk, $P < 0.05$; Kolmogorov–Smirnov test). Numbers in parentheses indicate the total number of growth cones examined. Error bars indicate standard error of the mean (s.e.m.).

© 2003 Nature Publishing Group

decreased, growth-cone turning induced by the netrin-1 gradient shifted from attraction to repulsion. A significant shift in turning behaviour was observed when one cyclic nucleotide was at least threefold in excess of the other, whereas a ninefold excess of [Sp-8-Br-cAMPS] or [8-Br-cGMP] ensured a significant attractive or repulsive response, respectively (Fig. 1d, see also Supplementary Information). The turning responses correlate with the ratio of cAMP and cGMP signalling: a high [cAMP]/[cGMP] ratio favours attraction, whereas a low ratio favours repulsion. Such second-messenger-dependent bi-directional behaviour is reminiscent of the dependence of synaptic potentiation/depression on stimulus frequency or postsynaptic Ca^{2+} levels, as described by the Bienenstock–Cooper–Munro theory of synaptic plasticity[10–12]. The dependence of growth-cone turning on the ratio of [cAMP] to [cGMP] could also account for the observations described earlier on DCC- and DCC–UNC5-mediated turning responses, and are consistent with the modulation of signal transduction pathways by these cyclic nucleotides.

How do cAMP and cGMP signalling pathways modulate netrin-1 signals? We have demonstrated previously that in *Xenopus* neurons, netrin-1-induced attraction requires Ca^{2+} entry through voltage-dependent Ca^{2+} channels (VDCCs) including LCCs[2], which are known to be activated by cAMP but inactivated by cGMP signalling pathways[13,14]. Recent studies of *Xenopus* neurons demonstrated that spontaneous Ca^{2+} spikes, which depend on Ca^{2+} entry through VDCCs and Ca^{2+} release through ryanodine receptors (RyRs)[15], correlate with transient changes in the intracellular concentration of cAMP[16]. Therefore, we measured Ca^{2+} channel activity by whole-cell voltage-clamp recordings of growth cones (Fig. 2a). In control growth cones, netrin-1 induced a marked increase in the amplitude of L-type Ca^{2+} currents, as revealed by the magnitude of nimodipine-sensitive (20 μM) inward currents observed in response to depolarizing voltage steps[17] in the presence of tetrodotoxin (TTX), caesium ions (Cs) and tetraethylammonium (TEA) (Fig. 2b, c, e; see Methods). These increases in Ca^{2+} currents were not observed at the soma in the presence of a netrin-1 gradient towards the growth cone (Fig. 2b; see also Supplementary Information). In contrast to that found in control neurons, netrin-1 significantly decreased Ca^{2+}

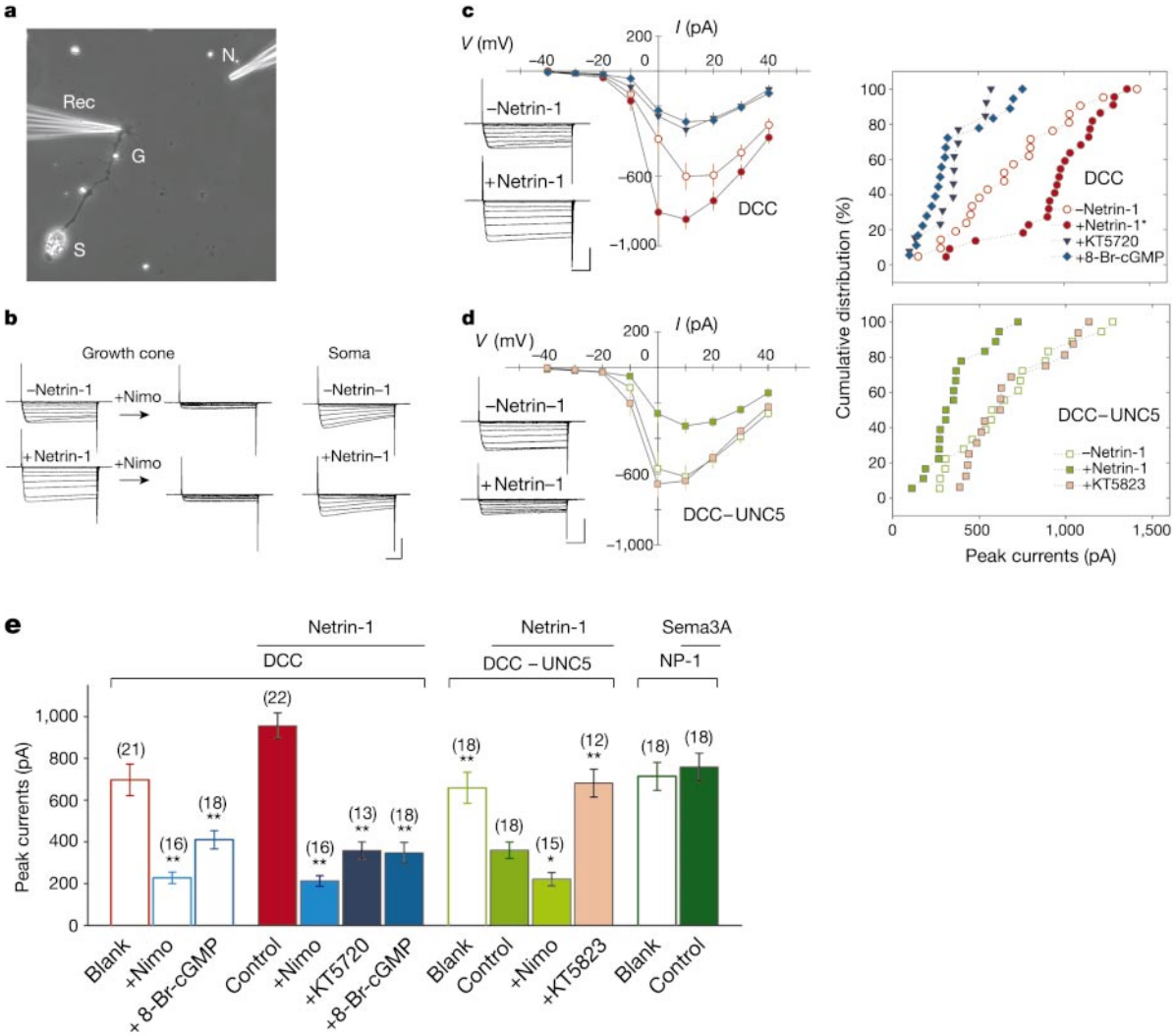

Figure 2 cAMP/cGMP signalling-dependent modulation of LCC activity induced by netrin-1. **a**, Phase-contrast image of a *Xenopus* spinal neuron. G, growth cone; S, soma; N, netrin-1 pipette; Rec, recording pipette. **b**, Sample traces of Ca^{2+} currents in response to voltage steps (−40 to +40 mV) in the absence (−netrin-1) or presence (+netrin-1) of a netrin-1 gradient, recorded from the growth cone before (left) and after (centre) addition of nimodipine (20 μM), or from the soma (right). **c**, **d**, Sample traces of Ca^{2+} currents (inset), summaries of *I/V* relationship (left) and cumulative distribution of the peak Ca^{2+} currents (right) measured in DCC and DCC–UNC5 neurons. **e**, Average peak amplitude of Ca^{2+} currents in DCC, DCC–UNC5 or NP-1 neurons in the absence or presence of a netrin-1 or Sema3A gradient. The column labelled 'blank' indicates no netrin-1 gradient. Significance test as in Fig. 1c. Scales; 500 pA, 20 ms.

© 2003 Nature Publishing Group

currents through LCCs in the growth cones of UNC5-overexpressing neurons (Fig. 2d, e). However, application of Sema3A had no effect on Ca^{2+} currents in these neurons (Fig. 2e). Notably, bath application of either 8-Br-cGMP or KT5720 reduced Ca^{2+} currents in control neurons either in the presence or absence of netrin-1 (Fig. 2c, e), similar to that found in netrin-1-treated UNC5-overexpressing neurons (Fig. 2d, e). Consistently, bath application of KT5823 significantly rescued Ca^{2+} currents in UNC5-overexpressing neurons (Fig. 2d, e). Thus, a constitutive level of cAMP signalling is required to maintain the basal activity of LCCs in control neurons. Moreover, conditions that trigger attractive or repulsive growth-cone turning were found to induce, respectively, enhanced or reduced Ca^{2+} currents in growth cones. The bi-directional modulation of growth-cone turning by cyclic nucleotide pathways thus directly reflects a modulation of LCC activity in response to netrin-1.

Modulation of ion channels induced by ligand-receptor activation is mediated by second messengers in a variety of neurons[18]. Serotonin-induced activation of *Aplysia* sensory neurons is mediated by cAMP signalling and is antagonized by the tetrapeptide FMRFamide through the action of the arachidonate 12-lipoxygenase metabolite 12-hydroperoxyeicosatetraenoic acid (12-HPETE)[19]. This antagonism is due to the converging actions of cAMP and 12-HPETE signalling pathways on the same K^+ channel[19]. Because 12-HPETE regulates the cGMP level by direct activation of soluble guanylate cyclase[3], and 12-lipoxygenase is expressed in mammalian neurons[20,21] and in *Xenopus* oocytes[22], we examined the possibility that 12-HPETE is a downstream effector of DCC–UNC5-mediated signalling. Application of exogenous 12-HPETE (500 nM) indeed converted the netrin-1-induced attraction to repulsion in control neurons (Fig. 3a, e), but had no significant effect on repulsion in UNC5-overexpressing neurons (Fig. 3c, e). Furthermore, it significantly reduced Ca^{2+} currents in growth cones of control neurons (Fig. 3b, f). Because a specific 12-lipoxygenase inhibitor, baicalein (10 μM), had no significant effect on netrin-1-induced attraction (Fig. 3a, e), the 12-HPETE–cGMP pathway did not seem to be activated by netrin-1 in control neurons. However, in neurons overexpressing UNC5, baicalein (10 μM) converted netrin-1-induced repulsion to attraction (Fig. 3c, e) and rescued the Ca^{2+} currents (Fig. 3d, f). Although it has been reported that 12-hydroxyeicosatetraenoic acid (12-HETE), a stable by-product of 12-HPETE, is involved in the collapse of rat sensory growth cones

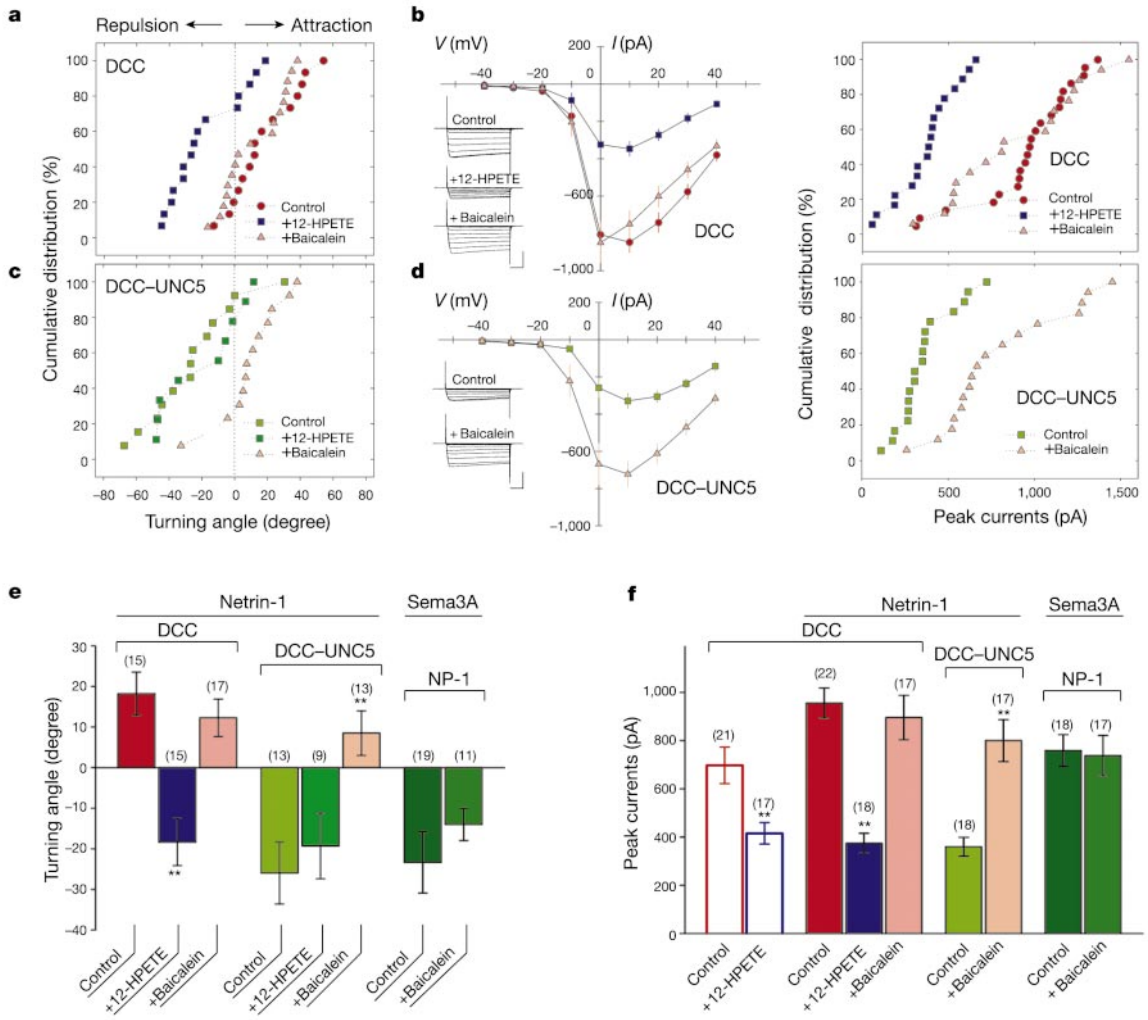

Figure 3 12-HPETE is required for DCC–UNC5-mediated repulsion. **a**, **c**, Distribution of turning angles in response to a netrin-1 gradient for DCC (**a**) and DCC–UNC5 (**c**) neurons in culture medium alone (control) or after addition of 12-HPETE or baicalein. **b**, **d**, Ca^{2+} currents in DCC (**b**) and DCC–UNC5 (**d**) neurons under the conditions described in **a**, **c**. **e**, Average turning angles in response to a netrin-1 or Sema3A gradient, for DCC, DCC–UNC5 or NP-1 neurons, under various conditions. **f**, Average peak amplitude of Ca^{2+} currents, corresponding to the experimental conditions described in **e**. Significance test as in Fig. 1c. Scales; 500 pA, 20 ms.

© 2003 Nature Publishing Group

induced by Sema3A (ref. 23), we found that baicalein treatment had no significant effect on NP-1-mediated repulsion, nor on growth-cone Ca^{2+} currents in the presence of Sema3A (Fig. 3e, f). These results suggest that 12-HPETE activates a cGMP-dependent pathway and is a specific downstream effector of DCC–UNC5 signalling, although a role for other metabolites cannot be excluded. These results provide further support for the hypothesis that distinct pathways underlie netrin-1- and Sema3A-induced repulsion.

Our findings suggest that modulation of Ca^{2+} channels through cyclic nucleotide-dependent signalling pathways may directly mediate netrin-1-induced bi-directional growth-cone guidance. Activation of DCC and DCC–UNC5 by netrin-1 may trigger two different cyclic nucleotide signalling pathways (Fig. 4). In our model, activation of DCC leads to activation of LCCs[2]. In the absence of UNC5, DCC activation also triggers a cAMP-dependent signalling pathway[6,24] and enhances LCC activity[13] (Fig. 4a). Enhanced Ca^{2+} entry, together with additional Ca^{2+} release from RyRs and inositol 1,4,5-trisphosphate receptors in the endoplasmic reticulum (ER)[25,26], creates a high-level gradient of intracellular Ca^{2+} concentration ($[Ca^{2+}]_i$) favouring growth-cone attraction[2]. In the presence of UNC5 (Fig. 4b), netrin-1 activation of DCC–UNC5 also triggers cGMP signalling, mediated by 12-HPETE. Activation of cGMP signalling results in a lower-level $[Ca^{2+}]_i$ gradient and growth-cone repulsion[2]. Thus, different spatial patterns of $[Ca^{2+}]_i$ at the growth cone are responsible for activating different sets of downstream effectors resulting in bi-directional turning responses. This notion is further supported by observations shown in Fig. 1. As shown in Fig. 4c, in DCC-expressing neurons, a netrin-1 gradient was attractive (high $[cAMP]_i/[cGMP]_i$ or $[Ca^{2+}]_i$) either under normal conditions or with PKG inhibition, but became repulsive when PKA activity was inhibited or when cGMP signalling was activated (low $[cAMP]_i/[cGMP]_i$ or $[Ca^{2+}]_i$). Conversely, in neurons overexpressing UNC5, netrin-1-induced activation of DCC–UNC5 leads to increased cGMP signalling (lower $[cAMP]_i/[cGMP]_i$ and $[Ca^{2+}]_i$) resulting in repulsion, which can be converted to attraction by PKG inhibition. Finally, in either DCC- or DCC–UNC5-expressing neurons, simultaneous inhibition of PKA activity (with KT5720) and activation of cGMP signalling (using either 8-Br-cGMP or activation of the DCC–UNC5 complex) resulted in an abrogation of netrin-1-induced turning, presumably because this combination suppresses Ca^{2+} signals altogether.

Our results strongly support the hypothesis that bi-directional turning responses of nerve growth cones to netrin-1 depend on the relative activities of cAMP- and cGMP-dependent pathways, which regulate the cytosolic level of Ca^{2+} signals by modulating Ca^{2+} channels in the plasma membrane and ER[2]. We also demonstrated a possible role for the lipid 12-HPETE as an effector of UNC5 signalling in triggering repulsive growth-cone turning. Our results show that the interaction of cyclic nucleotide and Ca^{2+} signalling pathways is critical in determining the direction of growth-cone extension, and that regulation of Ca^{2+} channels is a pivotal early event in the transduction of netrin-1 signals. □

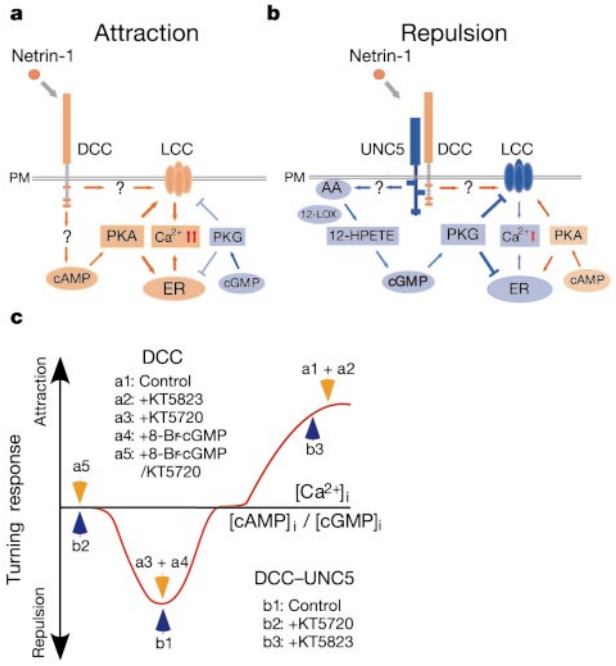

Figure 4 Model for netrin-1-induced second messenger signalling. **a**, For attraction, DCC activation by a netrin-1 gradient creates a high-level $[Ca^{2+}]_i$ gradient by triggering LCC activity and by stimulating the cAMP–PKA pathway, which further activates LCC in the plasma membrane (PM) and Ca^{2+} channels in the ER. **b**, For repulsion, activation of DCC–UNC5 by a netrin-1 gradient results in a low-level $[Ca^{2+}]_i$ gradient by triggering LCC activity and the arachidonic acid pathway, which in turn elevates 12-HPETE and cGMP, and consequently inactivates LCC and Ca^{2+} channels in the ER. **c**, Summary of $[cAMP]_i/[cGMP]_i$- and $[Ca^{2+}]_i$-dependent growth-cone turning responses to netrin-1.

Methods

In vitro transcription

Capped messenger RNAs were synthesized using mMESSAGE mMACHINE (Ambion) as described by the manufacturer. The transcription products were purified using the QIAquick PCR Purification Kit (Qiagen). The integrity of mRNAs was examined by agarose gel electrophoresis.

Xenopus microinjection and primary spinal neuron cultures

In vitro fertilization was performed as described[27]. *Unc5H2* mRNA was injected into two blastomeres of *Xenopus laevis* embryos at the four-cell stage. For each blastomere, we injected 4–8 nl of mRNA solution containing 0.125 $\mu g\,\mu l^{-1}$ *Unc5H2* and 0.25 $\mu g\,\mu l^{-1}$ green fluorescent protein (GFP) mRNA. GFP was used as an indicator for expression of the sample mRNA. Cultures of spinal neurons were prepared from neural tube tissues of stage 22 (for netrin-1 assays) and 26 (for Sema3A assays) *Xenopus* embryos, as described previously[2,4]. Cultures were used between 14–20 h after plating at room temperature (20–22 °C). Culture medium consisted of 49% (v/v) Leibovitz medium (GIBCO), 1% (v/v) fetal bovine serum (HyClone) and 50% (v/v) Ringer's solution (in mM: 115 NaCl, 2 $CaCl_2$, 2.5 KCl and 10 HEPES, pH 7.4).

Guidance proteins and pharmacological usage

Netrin-1 (5 $\mu g\,ml^{-1}$)[2,4], Sema3A protein (3,000 $U\,ml^{-1}$)[28] and 12-HPETE (500 nM)[29] were prepared as described. Agonists and antagonists were purchased from Calbiochem. The biological activity of Sema3A ($U\,ml^{-1}$) was evaluated using a collapse assay in chick DRG neurons[30]. All pharmacological agents, except 12-HPETE, were applied in the bath 30 min before experiments. 12-HPETE was applied in the bath 3 min before the turning assay (500 nM) or was used to generate a gradient (0.5 mM in the pipette) through a micropipette using pulsatile ejection during electrophysiological studies. Stability of 12-HPETE in the bath, as tested previously[29], was at least 6 min at 37 °C.

Growth-cone turning assay

Microscopic gradients of guidance proteins were produced as previously described[2,4]. Microscopic images of neurites were recorded with a CCD (charge-coupled device) camera (Hitachi KP-M2U) attached to a phase contrast microscope (Olympus CK-40) and analysed using NIH Image 1.62. The final turning angle, defined by the angle between the original direction of neurite extension and a straight line connecting the positions of the growth cone at the onset and the end of the 1-h period, was measured. Only those growth cones with net extension >7 μm over the 1-h period were included for analysis.

Electrophysiology

Whole-cell voltage-clamp recordings were made in *Xenopus* spinal neuron growth cones or soma using pipettes with resistances ranging from 5 to 8 MΩ or 4 to 6 MΩ, respectively, using a patch-clamp amplifier (Axopatch 200B, Axon). Recording pipettes were filled with an internal solution of (in mM): 115 CsCl, 10 HEPES, 10 TEA-Cl, 10 EGTA, 4 Mg-ATP, and was adjusted to pH 7.4 with CsOH. The bathing solution contained (in mM): 80 NaCl, 35 TEA-Cl, 10 $CaCl_2$, 10 HEPES, 1×10^{-6} TTX, and was adjusted to pH 7.4 with NaOH. A series resistance ≤15 MΩ was deemed acceptable, and was compensated by 40–50% with a 10-μs lag time. Whole-cell Ca^{2+} currents evoked by step depolarization from a holding

© 2003 Nature Publishing Group

potential of −40 mV to +40 mV (each step 10 mV for 100 ms)[17] were recorded with the patch-clamp amplifier. Data were filtered at 2 kHz and collected at 10 kHz. Ca^{2+} channel activity was evaluated by measuring peak inward currents.

Received 15 January; accepted 19 May 2003; doi:10.1038/nature01751.

1. Song, H.-J. & Poo, M.-m. Signal transduction underlying growth cone guidance by diffusible factors. *Curr. Opin. Neurobiol.* **9,** 355–363 (1999).
2. Hong, K., Nishiyama, M., Henley, J., Tessier-lavigne, M. & Poo, M.-m. Calcium signalling in the guidance of nerve growth by netrin-1. *Nature* **403,** 93–98 (2000).
3. Brune, B. & Ullrich, V. 12-Hydroperoxyeicosatetraenoic acid inhibits main platelet functions by activation of soluble guanylate cyclase. *Mol. Pharmacol.* **39,** 671–678 (1991).
4. Hong, K. *et al.* A ligand-gated association between cytoplasmic domains of UNC5 and DCC family receptors converts netrin-induced growth cone attraction to repulsion. *Cell* **97,** 927–941 (1999).
5. de la Torre, J. R. *et al.* Turning of retinal growth cones in a netrin-1 gradient mediated by the netrin receptor DCC. *Neuron* **19,** 1211–1224 (1997).
6. Ming, G. L. *et al.* Cyclic AMP-dependent growth cone guidance by netrin-1. *Neuron* **19,** 1225–1235 (1997).
7. Baldridge, W. H. & Fischer, A. J. Nitric oxide donor stimulated increase of cyclic GMP in the goldfish retina. *Vis. Neurosci.* **18,** 849–856 (2001).
8. Song, H.-j. *et al.* Conversion of neuronal growth cone responses from repulsion to attraction by cyclic nucleotides. *Science* **281,** 1515–1518 (1998).
9. Kolodkin, A. L. *et al.* Neuropilin is a Semaphorin III receptor. *Cell* **90,** 753–762 (1997).
10. Bienenstock, E. L., Cooper, L. N. & Munro, P. W. Theory for the development of neuron selectivity: orientation specificity and binocular interaction in visual cortex. *J. Neurosci.* **2,** 32–48 (1982).
11. Bear, M. F. Mechanism for a sliding synaptic modification threshold. *Neuron* **15,** 1–4 (1995).
12. Nishiyama, M., Hong, K., Mikoshiba, K., Poo, M.-m. & Kato, K. Calcium stores regulate the polarity and input specificity of synaptic modification. *Nature* **408,** 584–588 (2000).
13. Ruiz-Velasco, V., Zhong, J., Hume, J. R. & Keef, K. D. Modulation of Ca^{2+} channels by cyclic nucleotide cross activation of opposing protein kinases in rabbit portal vein. *Circ. Res.* **82,** 557–565 (1998).
14. Carabelli, V., D'Ascenzo, M., Carbone, E. & Grassi, C. Nitric oxide inhibits neuroendocrine Ca_v1 L-channel gating via cGMP-dependent protein kinase in cell-attached patches of bovine chromaffin cells. *J. Physiol.* **541,** 351–366 (2002).
15. Spitzer, N. C., Lautermilch, N. J., Smith, R. D. & Gomez, T. M. Coding of neuronal differentiation by calcium transients. *BioEssays* **22,** 811–817 (2000).
16. Gorbunova, Y. V. & Spitzer, N. C. Dynamic interactions of cyclic AMP transients and spontaneous Ca^{2+} spikes. *Nature* **418,** 93–96 (2002).
17. Lipsombe, D. *et al.* Spatial distribution of calcium channels and cytosolic calcium transients in growth cones and cell bodies of sympathetic neurons. *Proc. Natl Acad. Sci. USA* **85,** 2398–2402 (1988).
18. Greengard, P. The neurobiology of slow synaptic transmission. *Science* **294,** 1024–1030 (2001).
19. Piomelli, D. *et al.* Lipoxygenase metabolites of arachidonic acid as second messengers for presynaptic inhibition of *Aplysia* sensory cells. *Nature* **328,** 38–43 (1987).
20. Nishiyama, M. *et al.* Localization of arachidonate 12-lipoxygenase in canine brain tissues. *J. Neurochem.* **58,** 1395–1400 (1992).
21. Nishiyama, M., Watanabe, T., Ueda, N., Tsukamoto, H. & Wakanabe, K. Arachidonate 12-lipoxygenase is localized in neurons, glial cells and endothelial cells of the canine brain. *J. Histochem. Cytochem.* **41,** 111–117 (1993).
22. Hawkins, D. J. & Brash, A. R. Lipoxygenase metabolism of polyunsaturated fatty acids in oocytes of the frog *Xenopus laevis*. *Arch. Biochem. Biophys.* **268,** 447–455 (1989).
23. Mikule, K., Gatlin, J. C., de la Houssaye, B. A. & Pfenninger, K. H. Growth cone collapse induced by semaphorin 3A requires 12/15-lipoxygenase. *J. Neurosci.* **22,** 4932–4941 (2002).
24. Hopker, V. H., Shewan, D., Tessier-Lavigne, M., Poo, M.-m. & Holt, C. Growth-cone attraction to netrin-1 is converted to repulsion by laminin-1. *Nature* **401,** 69–73 (1999).
25. Hain, J., Onoue, H., Mayrleitner, M., Fleischer, S. & Schindler, H. Phosphorylation modulates the function of the calcium release channel of sarcoplasmic reticulum from cardiac muscle. *J. Biol. Chem.* **270,** 2074–2081 (1995).
26. Furuichi, T., Kohda, K., Miyawaki, A. & Mikoshiba, K. Intracellular channels. *Curr. Opin. Neurobiol.* **4,** 294–303 (1994).
27. Tabti, N. & Poo, M.-m. in *Culturing Nerve Cells* (eds Banker, G. & Goslin, K.) 137–154 (MIT Press, Cambridge, Massachusetts, 1991).
28. Sasaki, Y. *et al.* Fyn and Cdk5 mediate semaphorin-3A signaling, which is involved in regulation of dendrite orientation in cerebral cortex. *Neuron* **35,** 907–920 (2002).
29. Nishiyama, M. *et al.* Endothelium is required for 12-hydroperoxyeicosatetraenoic acid-induced vasoconstriction. *Eur. J. Pharmacol.* **341,** 57–63 (1998).
30. Goshima, Y. *et al.* A novel action of collapsing: collapsing-1 increases antero- and retrograde axoplasmic transport independently of growth cone collapse. *J. Neurobiol.* **33,** 316–328 (1997).

Supplementary Information accompanies the paper on **www.nature.com/nature**.

Acknowledgements We thank K. Kato for technical assistance and W. R. Jelinek for critical comments on the manuscript. This work was supported by grants from NIH NINDS and a Whitehead Fellowship (K.H.). M.T.L. is an investigator of the Howard Hughes Medical Institute.

Competing interests statement The authors declare that they have no competing financial interests.

Correspondence and requests for materials should be addressed to K.H. (hongk02@med.nyu.edu).

LAF1 ubiquitination by COP1 controls photomorphogenesis and is stimulated by SPA1

Hak Soo Seo, Jun-Yi Yang, Masaki Ishikawa, Cordelia Bolle, Maria L. Ballesteros & Nam-Hai Chua

Laboratory of Plant Molecular Biology, Rockefeller University, 1230 York Avenue, New York, New York 10021, USA

Far-red light regulates many aspects of seedling development, such as inhibition of hypocotyl elongation and the promotion of greening[1], acting in part through phytochrome A (phyA). The RING motif protein COP1 is also important because *cop1* mutants exhibit constitutive photomorphogenesis in darkness[2,3]. COP1 is present in the nucleus in darkness but is gradually relocated to the cytoplasm upon illumination[4]. Here we show that COP1 functions as an E3 ligase ubiquitinating both itself and the myb transcription activator LAF1, which is required for complete phyA responses[5]. In transgenic plants, inducible COP1 overexpression leads to a decrease in LAF1 concentrations, but is blocked by the proteasome inhibitor MG132. The coiled-coil domain of SPA1, a negative regulator of phyA signalling[6], has no effect on COP1 auto-ubiquitination but facilitates LAF1 ubiquitination at low COP1 concentrations. These results indicate that, in darkness, COP1 functions as a repressor of photomorphogenesis by promoting the ubiquitin-mediated proteolysis of a subset of positive regulators, including LAF1. After the activation of phyA, SPA1 stimulates the E3 activity of residual nuclear COP1 to ubiquitinate LAF1, thereby desensitizing phyA signals.

In plants, the light signal is perceived by different photoreceptors that activate a network of signalling intermediates to control the expression of hundreds of genes[7]. The phytochrome photoreceptor family regulates downstream responses by switching between biologically inactive and active forms in response to absorbing red or far-red light, respectively[8]. Several *Arabidopsis* mutants deficient in intermediates of the phyA signalling pathway have been identified. Some of these show reduced responses, whereas others are hypersensitive[9,10]. The COP/DET/FUS proteins have been proposed to act as negative regulators of photomorphogenic development because their loss-of-function mutants develop as light-grown plants in darkness[11]. Among these repressors, the RING motif protein COP1 seems to be a key regulator that interacts with components of the phyA signalling pathway such as HY5 (ref. 12) and SPA1 (ref. 13).

LAF 1 is a myb transcription activator that participates in the transmission of phyA signals to downstream responses; this activator is localized in nuclear bodies[5]. Because COP1 is also found in nuclear bodies[14], we asked whether the two proteins are localized together. To this end, we transiently expressed LAF1 tagged with yellow fluorescent protein (YFP) and COP1 tagged with cyan fluorescent protein (CFP) in onion epidermal cells. Figure 1a shows that the two proteins were indeed localized in the same nuclear bodies, although COP1 was also found in cytoplasmic regions not containing LAF1, which is strictly localized in the nucleus.

Similar experiments showed that SPA1 was distributed in the nucleus and the cytosol but it could be relocalized by COP1 to the same LAF1/COP1 nuclear bodies, which is consistent with an interaction between SPA1 and COP1 *in vitro*[13].

The co-localization of LAF1 and COP1 indicates that the two proteins might interact. To study this, we performed a pull-down of products translated *in vitro* by using maltose-binding protein (MBP) and MBP–COP1. Control experiments showed that MBP alone did not interact with any of the products translated *in vitro*. As expected, COP1 interacted with CIP8 (ref. 15) but not luciferase

© 2003 Nature Publishing Group